Modeling a Direct Contact Heat Recovery Process from Molten Salt Droplets in Various Gases for Thermochemical Hydrogen Production

SAMANE GHANDEHARIUN, MARC A. ROSEN, MARTIN AGELIN-CHAAB
Faculty of Engineering and Applied Science
University of Ontario Institute of Technology
2000 Simcoe St. N., Oshawa, ON, L1H 7K4
CANADA
samane.ghandehariun@uoit.ca, marc.rosen@uoit.ca, martin.agelin-chaab@uoit.ca

Abstract: The copper-chlorine cycle for hydrogen production is based on thermochemical water decomposition. Heat recovery within the cycle is necessary for high efficiency, and significant heat recovery can be achieved by cooling and solidifying the molten salt exiting the oxygen reactor step of the cycle. Heat can be recovered from the molten salt by breaking the molten stream into smaller dispersed droplets. A predictive model is developed here for direct contact heat recovery process from molten salt using various gases such as nitrogen, helium, argon and air. As CuCl may react with water vapor in the presence of oxygen, inert gases are considered as alternative coolants for the direct contact heat recovery process. It is observed that heat transfer is better for helium than the other gases considered.

Key-Words: hydrogen; thermochemical water decomposition; direct contact heat transfer; molten salt

1 Introduction

Hydrogen is considered a clean energy carrier if it is produced from clean energy sources [1-3]. Much of the hydrogen produced today is from fossil fuels, based on reforming or gasification processes [4, 5]. Thermochemical water decomposition cycles provide alternative and potentially more efficient methods to produce hydrogen from water [6].

A thermochemical water decomposition cycle decomposes water into hydrogen and oxygen using heat or, in a hybrid thermochemical cycle, a combination of heat and electricity. All the chemicals are used in a closed cycle so the net material outputs are oxygen and hydrogen.

Several thermochemical water decomposition cycles have been proposed and examined, including a solar energy-based two-step thermochemical cycle for hydrogen production based on a SnO_2/SnO redox reaction [7], a thermochemical cycle based on a Zn/ZnO redox reaction [8], a solar energy-based sulfur-iodine cycle for decomposing sulfuric acid [9], and a sulfur-iodine cycle for hydrogen production using nuclear energy [10].

Energy and economic assessments of an industrial plant for hydrogen production by a sulfur-iodine thermochemical cycle were presented by Liberatore et al. [11]. The energy efficiency of the thermochemical cycle based on the higher heat value was found to be 34% and, if electricity production is accounted for, including the efficiency of the solar plants, the total heat-to-hydrogen efficiency was found to be 21%. Recent advances in thermochemical cycles for hydrogen production, using non-fossil energy sources such as nuclear or solar, have been reported [12, 13].

Lewis et al. investigated various thermochemical cycles for hydrogen production and showed the copper-chlorine cycle to be chemically viable in terms of engineering factors and efficient [12]. The potential of the copper-chlorine cycle is in large part due to its lower temperature requirement for heat compared to most other thermochemical cycles. Heat recovery is important with such cycles for high efficiency

The objective of this paper is to improve understanding and assist efforts to design efficient and practical heat recovery systems for the Cu-Cl cycle. A predictive model is presented for direct contact heat recovery from molten salt CuCl using such gases as nitrogen, helium, argon and air.

2 Thermochemical Cycle

The copper-chlorine (Cu-Cl) cycle decomposes water into hydrogen and oxygen, through intermediate copper chloride compounds, in a closed loop that recycles all chemicals. Variations of the Cu-Cl cycle exist, based on the number of the main chemical reactions: three step, four step, and five step. These variations, all of which utilize

CuCl molten salt, have been compared in terms of major features [14]. Canadian advances in nuclear-based hydrogen production by the Cu-Cl cycle have been reported [15-18]. An analysis of a solar plant coupled with a Cu-Cl plant to produce hydrogen at three locations in Canada demonstrated the feasibility of the solar thermochemical Cu-Cl cycle for large-scale hydrogen production [19].

A schematic of a four step cycle is shown in Fig. 1. CuCl/HCl electrolysis (step 1) involves oxidation of copper(I) chloride (CuCl) in an electrochemical reaction, in the presence of hydrochloric acid (HCl), to produce hydrogen (H_2) and copper(II) chloride ($CuCl_2$). Drying (step 2) is where aqueous $CuCl_2$ exiting the electrolysis cell is dried to produce solid $CuCl_2$ particles. These particles enter hydrolysis (step 3) and are reacted with superheated steam to produce copper oxychloride solid (Cu_2OCl_2) and hydrochloric gas (HCl). Oxygen production (step 4) involves the decomposition of copper oxychloride particles into molten CuCl and O_2 gas.

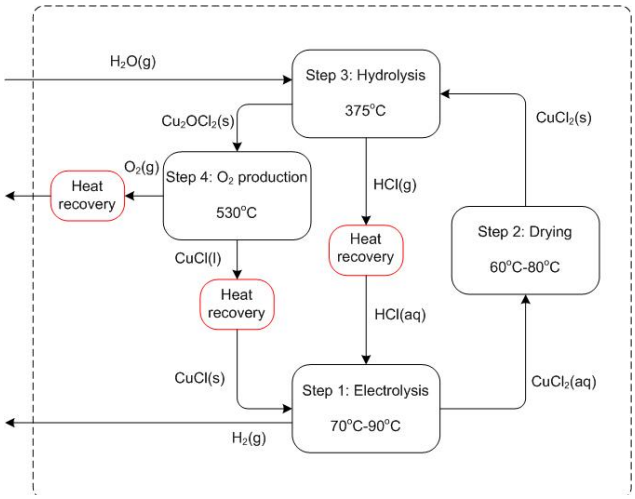

Fig. 1. Schematic of four step copper-chlorine cycle for hydrogen production via thermochemical water decomposition.

Heat recovery within the copper-chlorine cycle is important for efficiency and viability. Pinch analysis was used to determine the maximum recoverable heat within the Cu-Cl cycle, and the location in the cycle where recovered heat can be used efficiently [20]. It was shown that 88% of the heat recovery can be achieved by cooling and solidifying molten copper(I) chloride (CuCl) exiting the oxygen reactor, and that it is advantageous to use the recovered heat in hydrolysis.

Several configurations for heat recovery from molten CuCl, based on industrial processes for molten materials, have been investigated [21]. Two heat exchanger types were recommended: direct contact and indirect contact. Indirect contact heat recovery was analyzed elsewhere [22], with a counter-current air flow considered. The axial growth of the solid layer was presented, along with variations in the coolant and wall temperatures. Analytical and experimental investigation of direct contact heat recovery have been reported [23, 24], using air as a coolant. As CuCl may react with water vapor in the presence of oxygen, inert gases can be considered as potential coolants.

A predictive model is developed here for direct contact heat recovery from molten salt CuCl using such gases as nitrogen, helium, argon and air, to aid efforts to design efficient and practical heat recovery systems for the Cu-Cl cycle.

3 Direct Contact Heat Recovery

The acceleration and velocity of a freely-falling droplet is determined with Newton's second law as:

$$m_d\left(\frac{dv}{dt}\right) = m_d g\left(1-\frac{\rho_g}{\rho_d}\right) - \frac{1}{8}\pi d^2 \rho_g C_D v^2, \quad (1)$$

where m_d is the mass of the droplet, v is the droplet velocity, g is the gravitational acceleration, ρ_g is the ambient gas density, ρ_d is the droplet density, d is the droplet diameter, and C_D is the drag coefficient. The drag coefficient can be determined with the following correlation for $Re < 3\times10^5$ [25]:

$$C_D = \frac{24}{Re}(1+0.15Re^{0.687}) + \frac{0.42}{1+4.25\times10^4 Re^{-1.16}} \quad (2)$$

Here, Re is the Reynolds number, defined as $Re = vd/\nu_g$, where ν_g is the kinematic viscosity of the ambient gas.

Equation (1) is solved assuming a constant drag coefficient and for an initial condition $v(t) = 0$:

$$v(t) = v_t \tanh\left(\frac{g\left(1-\frac{\rho_g}{\rho_d}\right)t}{v_t}\right), \quad (3)$$

where v_t is the terminal velocity at which the weight of the droplet is balanced by the upward buoyancy and drag forces. That is,

$$v_t = \sqrt{\frac{4gd}{3C_D}\frac{(\rho_d - \rho_g)}{\rho_g}} \quad (4)$$

Equation (3) is integrated over time to find the vertical position as a function of time:

$$y(t) = \frac{v_t^2}{g\left(1-\frac{\rho_g}{\rho_d}\right)} ln\ cosh\left[\frac{g\left(1-\frac{\rho_g}{\rho_d}\right)t}{v_t}\right] \quad (5)$$

Heat transfer from a droplet occurs by three main mechanisms: convection, mass transfer, and radiative heat transfer. The convective heat transfer rate from the droplet can be expressed as:

$$\dot{q}_c = h_c A\left(T_{d,s} - T_\infty\right), \quad (6)$$

where A is the droplet surface area, $T_{d,s}$ and T_∞ are the droplet surface and ambient gas temperatures, respectively, and h_c is the convection heat transfer coefficient, expressible as:

$$h_c = \frac{Nu\ k_g}{d}, \quad (7)$$

where Nu is the Nusselt number, and k_g is the thermal conductivity of the ambient gas. Various correlations have been proposed for the average Nusselt number for flow over a sphere. The following comprehensive correlation is used here [26]:

$$Nu = 2 + \left[0.4Re^{\frac{1}{2}} + 0.06Re^{\frac{2}{3}}\right] Pr^{0.4}\left(\frac{\mu_\infty}{\mu_s}\right)^{\frac{1}{4}}, \quad (8)$$

where Pr is the Prandtl number. This correlation is valid for $3.5 \leq Re \leq 80{,}000$ and $0.7 \leq Pr \leq 380$, and fluid properties are evaluated at the free-stream temperature, T_∞, except for μ_s which is evaluated at the surface temperature T_s.

The heat transfer rate due to mass transfer is given by [27]:

$$\dot{q}_m = Lh_m A(\rho_{v,s} - \rho_{v,\infty}), \quad (9)$$

where L is the latent heat of phase change (evaporation or sublimation), $\rho_{v,s}$ and $\rho_{v,\infty}$ are the vapor density at the droplet surface and away from the surface, respectively, and h_m is the mass transfer coefficient, expressed as:

$$h_m = \frac{Sh\ D_{vg}}{d}, \quad (10)$$

where Sh is the Sherwood number, and D_{vg} is the vapor-gas mass diffusivity. The Sherwood number is calculated using the Ranz-Marshall equation [28]:

$$Sh = 2 + 0.6Re_d^{\frac{1}{2}}Sc^{\frac{1}{3}} \quad (11)$$

where Sc is the Schmidt number, defined as: $Sc=\mu_g/\rho_g D_{vg}$

The radiation heat transfer rate from the droplet surface is:

$$\dot{q}_r = \varepsilon\sigma A(T_{d,s}^4 - T_\infty^4), \quad (12)$$

where ε is the emissivity of the surface and σ is the Stefan-Boltzmann constant (5.67×10^{-8} W/m^2.K^4).

Two models may be used for the droplet temperature: non-mixing and complete-mixing [29]. The non-mixing model assumes no internal motion in the droplet and the energy equation is reduced to that for transient heat conduction. A one-dimensional model can be used assuming the droplet shape to be constant and spherical. The one-dimensional transient heat conduction equation in a spherical droplet is expressed as [30]:

$$\rho_d c_{p,d}\frac{\partial T}{\partial t} = \frac{\partial}{\partial r}\left(k_d\frac{\partial T}{\partial r}\right) + \frac{2k_d}{r}\left(\frac{\partial T}{\partial r}\right), \quad (13)$$

where the initial and boundary conditions are:

$$T(r,0) = T_i \quad (14)$$

$$\left.\frac{\partial T}{\partial r}\right|_{r=0} = 0 \quad (15)$$

$$-k_d A_d \left.\frac{\partial T}{\partial r}\right|_{r=R} = \dot{q}_c + \dot{q}_m + \dot{q}_r \quad (16)$$

Here, $\dot{q}_c$, $\dot{q}_m$, and $\dot{q}_r$ represent heat transfer due to convection, mass transfer, and radiation, respectively. The solution to Eq. (13), for convection boundary conditions, is:

$$T^* = \sum_{n=1}^{\infty} C_n exp(-\zeta_n^2 Fo)\frac{1}{\zeta_n r^*}\ sin\ (\zeta_n r^*), \quad (17)$$

where Fo is the Fourier number defined as: $Fo=\alpha t/r_0^2$, and T^* and r^* are the dimensionless temperature and spatial coordinates, respectively, defined as:

$$T^* = \frac{T - T_\infty}{T_i - T_\infty} \quad (18)$$

$$r^* = \frac{r}{R} \quad (19)$$

Here, T_i is the initial temperature, T_∞ is the ambient temperature, and R is the droplet radius.

Discrete values of ζ_n are positive roots of the following transcendental equation which can be found in Ref. [30]:

$$1 - \zeta_n cot\, \zeta_n = Bi \tag{20}$$

The values of coefficients C_n are determined from:

$$C_n = \frac{4(sin\zeta_n - \zeta_n cos\zeta_n)}{2\zeta_n - \sin(2\zeta_n)} \tag{21}$$

The first six term of the series solution, Eq. (17), are used to approximate the temperature profile in the droplet. The maximum error caused by the six-term approximation is less than 7% for $Fo = 0$ and the accuracy improves with an increase in the Fourier number.

The complete-mixing model assumes internal motion of the droplet is sufficiently strong that mixing is complete. The temperature profile in the droplet is then essentially flat and resistance to heat transfer exists only in the surrounding gas. Assuming a uniform droplet temperature, the temperature change rate can be described by the heat balance between the droplet and the surrounding gas:

$$m_d c_{p,d} \frac{dT_d}{dt} = -(\dot{q}_c + \dot{q}_m + \dot{q}_r) \tag{22}$$

These two models represent the bounds on the droplet temperature. The actual temperature profile of the droplet is expected to lie between these two models.

4 Results and Discussion

Figure 2 illustrates the variation of the drag coefficient versus flight time for various gases. The drag coefficient varies with flight time because it is a function of velocity. Helium has a kinematic viscosity of about ten times higher than that of nitrogen or argon. Therefore, the Reynolds number in helium is lower and the drag coefficient is higher than for the other gases examined. As expected, the behavior with nitrogen is similar to that for air.

Figure 3 shows the acceleration of a falling droplet. Initially, the acceleration is equal to gravitational acceleration, but it decreases with flight time as drag force rises. The density of helium is one order of magnitude smaller than that of other gases, so the corresponding drag force is smaller and the droplet acceleration is greater in helium.

Figure 4 shows the velocity of the droplet versus the flight distance. The droplet initially has no velocity and it accelerates as it moves downward. As the droplet velocity increases with the falling distance, the Reynolds number increases. The droplet velocity is greater in helium. Buoyancy has been shown to have a negligible effect on the droplet velocity [24].

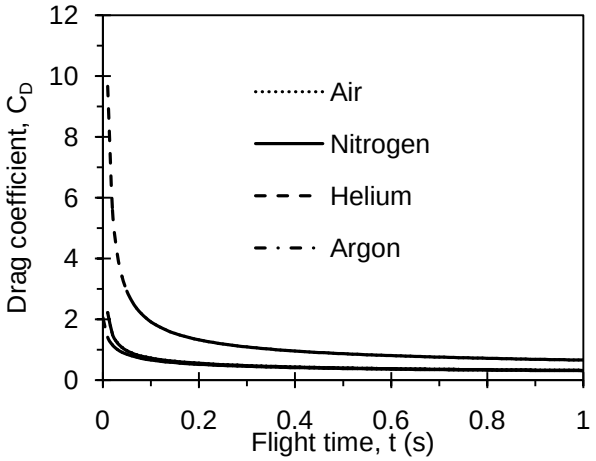

Fig. 2. Drag coefficient versus flight time.

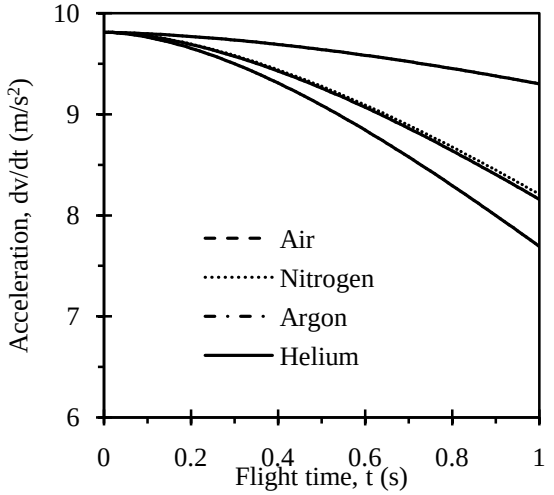

Fig. 3. Droplet acceleration versus flight time.

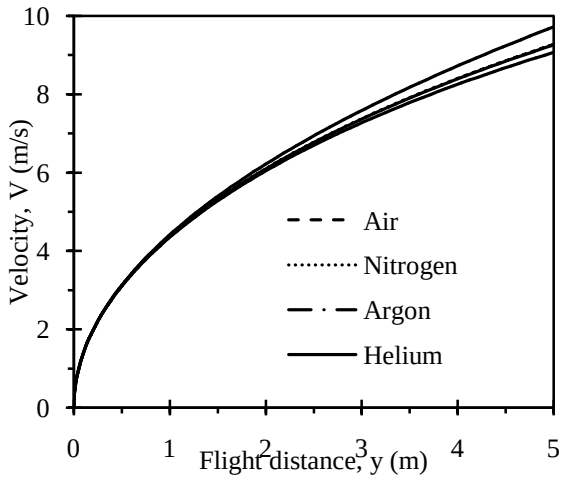

Fig. 4. Velocity of the falling droplet versus flight distance.

Figure 5 illustrates the variation in convection heat transfer coefficient during the flight. The velocity, Reynolds number, Nusselt number, and the heat transfer coefficient all increase as the droplet falls, except after the droplet reaches its terminal velocity.

As the droplet accelerates, the Reynolds number, and hence the convection heat transfer coefficient, increases rapidly causing a significant rise in the convection heat transfer rate. After, the rate of convection heat transfer is dominated by the temperature difference between the droplet surface and the ambient gas, and decreases with the flight time. However, the rate of radiation heat transfer decreases as the droplet surface temperature drops during flight. Mass transfer has been shown to have a negligible effect on the total heat transfer from the droplet [24].

Fig. 6 shows the surface temperature of the droplet versus the flight time in various gases, for an assumed ambient temperature of 21^{o}C. The initial temperature of the droplets is 504^{o}C. As the rate of heat transfer is greater in helium, the variation of droplet temperature is more significant.

5 CONCLUSIONS

Significant heat recovery can be achieved in the copper-chlorine cycle of hydrogen production by cooling and solidifying the CuCl molten salt exiting the oxygen reactor of the cycle. Heat can be recovered from the molten salt by breaking the molten stream into smaller dispersed droplets. A predictive analytical model is developed for a direct contact system for heat recovery from molten CuCl using various gases. As CuCl may react with oxygen, various inert gases are considered. Higher accelerations and hence higher heat transfer rates are observed for the droplets falling in helium. Therefore, the rates of change in droplet temperature are greater in helium than other considered gases. The results can help improve the efficiency the copper-chlorine cycle for hydrogen production of by improving heat recovery within the cycle.

Acknowledgement

Financial support from the Natural Sciences and Engineering Research Council of Canada (NSERC), the Ontario Research Fund (ORF), and Atomic Energy of Canada Limited (AECL) is gratefully acknowledged.

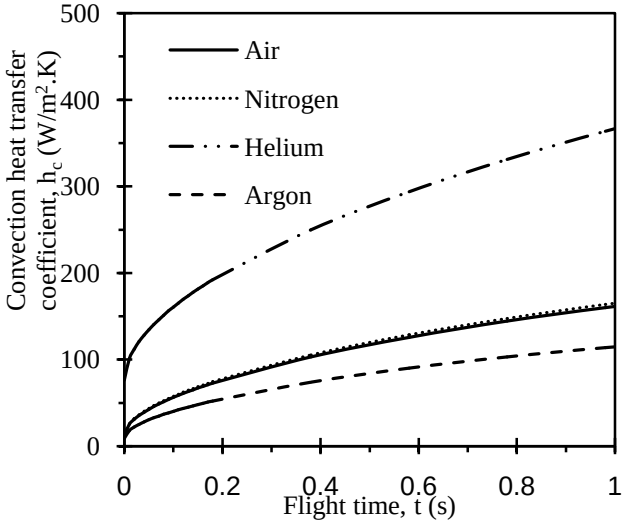

Fig. 5. Convection heat transfer coefficient versus flight time.

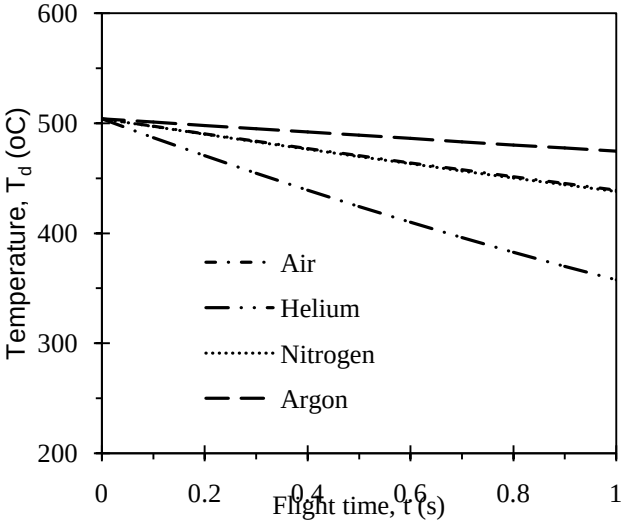

Fig. 6. Droplet temperature versus flight time

Nomenclature

A area, m^2
C_D drag coefficient
c_p specific heat at constant pressure, J/kg.K
Fo Fourier number
g gravitational acceleration, m/s^2
h heat transfer coefficient, $W/m^2.K$
L latent heat of phase change, kJ/kg
m mass, kg
Nu Nusselt number
Pr Prandtl number
q heat transfer rate, W
R droplet radius, m
r radial coordinate, m
Re Reynolds number
Sc Schmidt number
Sh Sherwood number
T temperature, ^oC
t time, s
v velocity, m/s

Greek Letters

ε emissivity
ζ_n positive roots of transcendental equation
μ_∞ viscosity of fluid at the free-stream temperature, Pa.s
ν_g kinematic viscosity of gas, m^2/s
ρ density, kg/m^3
ρ_g density of gas, kg/m^3
σ Stefan-Boltzmann constant (5.67×10^{-8} $W/m^2.K^4$)

Subscripts

c convection
d droplet
g gas
i initial
m mass transfer
r radiation
s surface

Superscripts

* non-dimensional

References:

[1] P. Moriarty, D. Honnery. 2009. Hydrogen's role in an uncertain energy future. *International Journal of Hydrogen Energy* 34: 31-39.

[2] A. Midilli, M. Ay, I. Dincer, M. A. Rosen. 2005. On hydrogen and hydrogen energy strategies I: current status and needs. *Renewable and Sustainable Energy Reviews* 9: 255-271.

[3] J. Nowotny, T. N. Veziroglu. 2011. Impact of hydrogen on the environment. *International Journal of Hydrogen Energy* 36: 3218-3224.

[4] R. Dell. 2004. *Clean energy*. London: Royal Society of Chemistry.

[5] R. Kothari, D. Buddhiand, R. L. Sawhney. Comparison of environmental and economic aspects of various hydrogen production methods. *Renewable and Sustainable Energy Reviews* 12: 553-563.

[6] J. E. Funk. 2001. Thermochemical hydrogen production: past and present. *International Journal of Hydrogen Energy* 26: 185-190.

[7] S. Abanades, P. Charvin, F. Lemont, G. Flamant. 2008. Novel two-step SnO_2/SnO water-splitting cycle for solar thermochemical production of hydrogen. *International Journal of Hydrogen Energy* 33: 6021-6030.

[8] A. Steinfeld, 2002. Solar hydrogen production via a two-step water splitting thermochemical cycle based on Zn/ZnO redox reactions. *International Journal of Hydrogen Energy* 27: 611-619.

[9] C. Huang, A. T. Raissi. 2005. Analysis of sulfur iodine thermochemical cycle for solar hydrogen production. Part I: Decomposition of sulfuric acid. *Solar Energy* 78: 632-646.

[10] W. Xinxin, O. Kaoru. 2005. Thermochemical water splitting for hydrogen production utilizing nuclear heat from an HTGR. *Tsinghua Science and Technology* 10:270–6.

[11] R. Liberatore, M. Lanchi, A. Giaconia, P. Tarquini. 2012. Energy and economic assessment of an industrial plant for the hydrogen production by watersplitting through the sulfur–iodine thermochemical cycle powered by concentrated solar energy. *International Journal of Hydrogen Energy* 37:9550–65.

[12] M. A. Lewis, J. G. Masin, P. A. O'Hare. 2009. Evaluation of alternative thermochemical cycles, Part I: The methodology, *International Journal of Hydrogen Energy* 34: 4115-4124.

[13] M. A. Rosen. 2010. Advances in hydrogen production by thermochemical water decomposition: A review. *Energy* 35: 1068-1076.

[14] A. L. Wang, G. F. Naterer, K. S. Gabriel, R. Gravelsins, V. N. Daggupati. 2009. Comparison of different copper-chlorine thermochemical cycles for hydrogen production. *International Journal of Hydrogen Energy* 34: 3267-3276.

[15] G. F. Naterer, S. Suppiah, L. Stolberg, M. Lewis, M. Ferrandon, Z. Wang, I. Dincer, K. Gabriel, M. A. Rosen, E. Secnik, E. B. Easton, L. Trevani, I. Pioro, P. Tremaine, S. Lvov, and J. Jiang, G. Rizvi, B. M. Ikeda, L. Lu, M. Kaye, W. R. Smith, J. Mostaghimi, P. Spekkens, M. Fowler, J. Avsec. 2011. Clean hydrogen production with the Cu-Cl cycle – Progress of international consortium, I: Experimental unit operations. *International Journal of Hydrogen Energy* 36: 15472-15485.

[16] G. F. Naterer, S. Suppiah, L. Stolberg, M. Lewis, M. Ferrandon, Z. Wang, I. Dincer, K. Gabriel, M. A. Rosen, E. Secnik, E. B. Easton, L. Trevani, I. Pioro, P. Tremaine, S. Lvov, and J. Jiang, G. Rizvi, B. M. Ikeda, L. Lu, M. Kaye, W. R. Smith, J. Mostaghimi, P. Spekkens, M. Fowler, J. Avsec. 2011. Clean hydrogen production with the Cu-Cl cycle – Progress of international consortium, II: Simulations, thermochemical data and materials. *International Journal of Hydrogen Energy* 36: 15486-15501.

[17] G. F. Naterer, S. Suppiah, L. Stolberg, M. Lewis, Z. Wang, I. Dincer, M. A. Rosen, K. Gabriel, E. Secnik, E. B. Easton, I. Pioro, S. Lvov, J. Jiang, J. Mostaghimi, B. M. Ikeda, G. Rizvi, L. Lu, A. Odukoya, P. Spekkens, M. Fowler, J. Avsec. 2013. Progress of international hydrogen production network for the thermochemical Cu–Cl cycle. *International Journal of Hydrogen Energy* 38: 740-759.

[18] G. F. Naterer, S. Suppiah, L. Stolberg, M. Lewis, Z. Wang, M. A. Rosen, I. Dincer, K. Gabriel, A. Odukoya, E. Secnik, E. B. Easton, V. Papangelakis. 2015. Progress in thermochemical hydrogen production with copper-chlorine cycle. *International Journal of Hydrogen Energy* 40: 6283-6295.

[19] S. Ghandehariun, G. F. Naterer, I. Dincer, M. A. Rosen. 2010. Solar thermochemical plant analysis for hydrogen production with copper-chlorine cycle. *International Journal of Hydrogen Energy* 35: 8511-8520.

[20] S. Ghandehariun, M. A. Rosen, G. F. Naterer, Z. Wang. 2012. Pinch analysis for recycling thermal energy in the Cu-Cl cycle. *International Journal of Hydrogen Energy* 37: 16535-16541.

[21] S. Ghandehariun, M. A. Rosen, G. F. Naterer, Z. Wang. 2011. Comparison of molten salt heat recovery options in the Cu-Cl cycle of hydrogen production. *International Journal of Hydrogen Energy* 36: 11328-11337.

[22] S. Ghandehariun, G. F. Naterer, M. A. Rosen, Z. Wang. 2014. Indirect contact heat recovery with solidification in thermochemical hydrogen production. *Energy Conversion and Management* 82: 212-218.

[23] S. Ghandehariun, Z. Wang, G. F. Naterer, M. A. Rosen. 2015. Experimental investigation of molten salt droplet quenching and solidification processes of heat recovery in thermochemical hydrogen production *Applied Energy* 157: 267-275.

[24] S. Ghandehariun, M. A. Rosen, G. F. Naterer. 2016. Direct contact heat transfer from molten salt droplets in a thermochemical water splitting process of hydrogen production *International Journal of Heat and Mass Transfer* 96: 125-131.

[25] R. Clift, M. E. Weber, J. R. Grace. 1978. *Bubbles, drops, and particles.* New York: Academic Press.

[26] S. Whitaker. 1972. Forced convection heat transfer correlations for flow in pipes, past flat plates, single cylinders, single spheres, and for flow in packed beds and tube bundles. *AIChE Journal* 18: 361-370.

[27] Y. A. Cengel. 2003. *Heat transfer: A practical approach.* New York: McGraw-Hill.

[28] W. Ranz, W. Marshall. 1952. Evaporation from drops. *Chemical Engineering Progress* 48: 141-146.

[29] S. C. Yao, V. E. Schrock. 1976. Heat and mass transfer from freely falling drops. *Journal of Heat Transfer* 98: 120-126.

[30] F. P. Incropera, D. P. DeWitt. 2001. *Fundamentals of heat and mass transfer*. New York: John Wiley & Sons.